


# Spatial transcriptomes within the *Pseudomonas aeruginosa* biofilm architecture

Yun Heacock-Kang <sup>1</sup>, Zhenxin Sun,<sup>1</sup>  
Jan Zarzycki-Siek,<sup>1</sup> Ian A. McMillan,<sup>1,2</sup>  
Michael H. Norris,<sup>1†</sup> Andrew P. Bluhm,<sup>1</sup>  
Darlene Cabanas,<sup>1</sup> Dawson Fogen,<sup>1</sup> Hung Vo,<sup>1</sup>  
Stuart P. Donachie,<sup>1</sup> Bradley R. Borlee,<sup>3</sup>  
Christopher D. Sibley,<sup>4</sup> Shawn Lewenza,<sup>4</sup>  
Michael J. Schurr,<sup>5</sup> Herbert P. Schweizer<sup>6</sup> and  
Tung T. Hoang<sup>1,2\*</sup>

<sup>1</sup>Department of Microbiology, University of Hawaii at Manoa, Honolulu, HI, USA.

<sup>2</sup>Department of Molecular Biosciences and Bioengineering, University of Hawaii at Manoa, Honolulu, HI, USA.

<sup>3</sup>Department of Microbiology, Immunology, and Pathology, Colorado State University, Fort Collins, CO, USA.

<sup>4</sup>Department of Microbiology, Immunology and Infectious Diseases, University of Calgary, Calgary, Canada.

<sup>5</sup>Department of Immunology and Microbiology, University of Colorado, Aurora, CO, USA.

<sup>6</sup>Department of Molecular Genetics and Microbiology, University of Florida, Gainesville, FL, USA.

## Summary

**Bacterial cooperative associations and dynamics in biofilm microenvironments are of special interest in recent years. Knowledge of localized gene-expression and corresponding bacterial behaviors within the biofilm architecture at a global scale has been limited, due to a lack of robust technology to study limited number of cells in stratified layers of biofilms. With our recent pioneering developments in single bacterial cell transcriptomic analysis technology, we generated herein an unprecedented spatial transcriptome map of the mature *in vitro* *Pseudomonas aeruginosa* biofilm model, revealing contemporaneous yet altered bacterial behaviors at different layers within the**

**biofilm architecture (i.e., surface, middle and interior of the biofilm). Many genes encoding unknown functions were highly expressed at the biofilm-solid interface, exposing a critical gap in the knowledge of their activities that may be unique to this interior niche. Several genes of unknown functions are critical for biofilm formation. The *in vivo* importance of these unknown proteins was validated in invertebrate (fruit fly) and vertebrate (mouse) models. We envisage the future value of this report to the community, in aiding the further pathophysiological understanding of *P. aeruginosa* biofilms. Our approach will open doors to the study of bacterial functional genomics of different species in numerous settings.**

## Introduction

Several examples of bacterial biofilms in both nature and clinically relevant settings have been presented in recent years (Costerton *et al.*, 1995; Lappin-Scott *et al.*, 2014). Biofilms exist in various niches in humans, including oral cavities, the genitalia, and the gut, where they may constitute a vital part of host-associated microbial communities (Filoche *et al.*, 2010; Danielsson *et al.*, 2011; Macfarlane *et al.*, 2011). Moreover, biofilm infections are notoriously difficult to treat because of increased tolerance to antimicrobial agents (Mah and O'Toole, 2001; Davies, 2003; Van Acker *et al.*, 2014). Bacterial behaviors and dynamics in biofilm microenvironments are of special interest in the field, and recent discoveries have begun to reveal exciting aspects of biofilm physiology and structure (Stewart and Franklin, 2008; Flemming and Wingender, 2010; Lappin-Scott *et al.*, 2014). Biofilm communities are physiologically distinct from their planktonic counterparts and, structurally, biofilm is a heterogeneous organization of bacteria. The mechanisms that contribute to genetic and physiological heterogeneity in biofilm are believed to include the genotypic variation that occurs through mutation and selection, as well as micro-scale chemical gradients and adaptation to local environmental conditions, which lead to differences in gene-regulation and -expression (Xu *et al.*, 1998; Boles *et al.*, 2004).

Accepted 12 October, 2017. \*For correspondence. E-mail tongh@hawaii.edu; Tel. (+808) 956 3522; Fax (+808) 956 5339. <sup>†</sup>Present address: Department of Infectious Diseases and Pathology, University of Florida, Gainesville, FL, USA.

© 2017 The Authors. *Molecular Microbiology* Published by John Wiley & Sons Ltd.

This is an open access article under the terms of the Creative Commons Attribution-NonCommercial-NoDerivs License, which permits use and distribution in any medium, provided the original work is properly cited, the use is non-commercial and no modifications or adaptations are made.

*P. aeruginosa* is an opportunistic pathogenic bacterium responsible for both acute and chronic infections. Its natural resistance to many antimicrobial compounds and its ability to form biofilms in various environments and produce many virulence factors makes *P. aeruginosa* an important human pathogen, particularly in immunocompromised individuals (Doring, 1997; Kipnis *et al.*, 2006). Additionally, *P. aeruginosa* has a complex network of genes that responds to different conditions to constantly adapt to environmental changes. With all these characteristics, *P. aeruginosa* has been a model organism for the investigation of biofilm and pathogenesis. Previous studies pioneered functional genomic approaches to study *P. aeruginosa* in the biofilm setting (Whiteley *et al.*, 2001; Williamson *et al.*, 2012), presenting some interesting aspects of localized gene-expression patterns. However, these studies utilized the entire biofilm structure or very large sections for transcriptomic analyses, lacking spatial resolution. With our recent developments in single bacterial cell transcriptomic analysis technology (Kang *et al.*, 2011; 2015), we aimed at an in-depth transcriptomic characterization of three distinct locations with the biofilm architecture (i.e., surface, middle and interior of the biofilm structure). An organized spatial gene-expression pattern of thousands of genes was unveiled for the surface, middle, and interior of the mature biofilm that make up the live and functioning biofilm as a whole.

## Results

### Stratified gene-expression within the vertical biofilm structure

Distinct spatial regions in mature biofilms (Fig. 1A) were characterized by reproducible (Supporting Information

Fig. S1A) and spatially dynamic patterns of gene-expression (Fig. 1B). A total of 2504 differentially expressed genes were detected in all three regions, and could thus be cross-compared. This covered 45% of genes in the *P. aeruginosa* genome, yielding higher resolution compared to the pioneering study which showed 1% of the genes are regulated in the biofilm (Whiteley *et al.*, 2001). We attributed this higher resolution of our approach to structurally dissect the biofilm for spatial transcriptome analysis, as variations in gene-expression can be canceled out when cells from different vertical locations are mixed together. Using gene-expression of planktonic cells as a baseline, our data showed active gene-expression in all spatial regions (Fig. 1B, Supporting Information Figs S1 and S2). A different approach for gene-expression analysis was also employed, using the average gene expression profile of the whole biofilm instead of the planktonic cells as control (Supporting Information Fig. S3). This list (Supporting Information Fig. S3) shared majority of the significant genes with Supporting Information Fig. S2, however, is more condensed and allows for easy visualization/identification of genes and operons that are differentially expressed in one location of the biofilm architecture versus the whole biofilm community. For consistency, data presented in Supporting Information Fig. S2 (planktonic control) will be used exclusively for the remainder of this study.

A gradient of elevated number of genes expressed near the surface and down-regulation of number of genes expressed toward the interior was observed (Supporting Information Fig. S1A). Although differential gene-expression was shown in all spatial regions in Supporting Information Fig. S1B, the type of genes expressed in each region differed markedly. KEGG

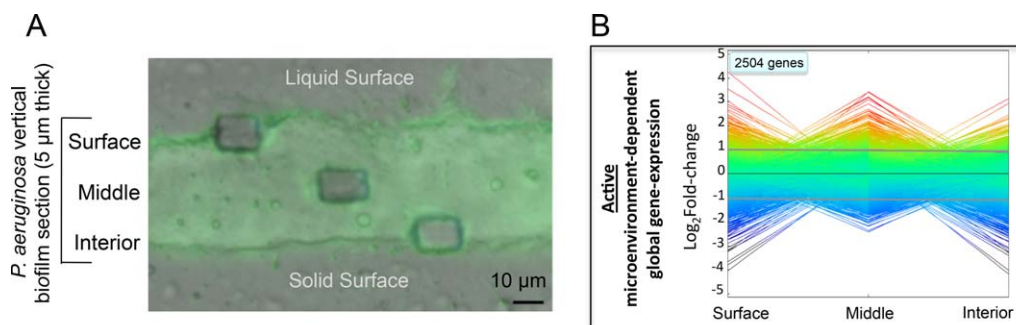


**Fig. 1.** Spatial gene-expression in the *P. aeruginosa* biofilm.

A. A GFP-tagged *P. aeruginosa* strain was used to grow biofilm on stainless steel coupons. After 72 h growth, the biofilm was fixed, embedded in Tissue-Tek OCT compound, and vertically sectioned. The Zeiss PALM system was used to isolate approximately  $150 \mu\text{m}^2$  sections from the surface, middle, and interior portions of the biofilm. Scale bar is  $10 \mu\text{m}$ . Three biological replicates of the sections were obtained in each spatial location.

B. Linear expression map of all genes detected from different locations in the biofilm. Each line represents a single gene, with the rainbow colors (red to purple) indicating positive to negative  $\log_2$  fold-change values. Genes above the line of  $\log_2$  fold-change = 1 are considered up-regulated, whereas genes below the line of  $\log_2$  fold-change = -1 are considered down-regulated in the biofilm compared to those in planktonically growing cells.

pathway mapping data (Data S1) provided easy visualization of all active pathways in three vertical locations within the biofilm. While the genome only encodes for approximately 25% of proteins with unknown functions, transcriptome data showed a large majority of differentially expressed genes (60–70%) have no homologs amongst any known genes/motifs (Supporting Information Fig. S1C; unknown category). This significant bias in the gene-expression data toward unknown proteins emphasizes how much we have yet to discover regarding functions of the bacterial community in the stratified biofilm.

#### *Localized pathophysiological and resistance behavior differences indicated by gene-expression*

Our approach identified spatially dependent global physiological variation in the mature biofilm. We extensively validated the transcriptome data by GFP-fusion and microscopy (Supporting Information Fig. S4), including examples of genes for which only limited data exist in one of the biological triplicates (Supporting Information Fig. S4C). Variations in expression levels were observed among different genes in the same operon (e.g., *psl* and *psc* operons), likely resulted from amplification bias using limited amount of bacteria transcripts as template. However, all genes/operons validated (29 total) showed the same trends between GFP fusion microscopy and transcriptome data (Supporting Information Fig. S4). All major biofilm matrix components (*alg*, *pel* and *psl* operons) were highly expressed by cells on the biofilm surface (Supporting Information Fig. S4A), which function as a physical barrier, and has also been shown to confer antibiotic tolerance (Colvin *et al.*, 2011; Tseng *et al.*, 2013; Billings *et al.*, 2013). Numerous antibiotic resistance mechanisms to counteract antimicrobial agents, including efflux-pumps, were also up-regulated on the biofilm surface (Supporting Information Fig. S4B). Since no antibiotics were present in the growth media, we reasoned that these efflux pumps were up-regulated by other mechanisms, such as quorum sensing. The combined expression of important biofilm matrix components (*alg*, *pel* and *psl* operons) and resistance genes highlight the reason for significant resistance to multiple drugs by *P. aeruginosa* in the biofilm mode of growth versus planktonic cells. Genes controlling quorum sensing regulation (Davies *et al.*, 1998) were differentially expressed (Supporting Information Fig. S2, *lasR*, PA1430; *rhlR*, PA3477), leading to distinct spatial expression of many downstream pathways (Supporting Information Fig. S4A and B). Among these, many established virulence gene/pathways were highly expressed on the surface of the biofilm (Supporting Information Fig. S4A), including LPS (PA3145–3160),

type III secretion system (PA1690–1723), effector ExoT (PA0044), exotoxin (ToxA, PA1148), phospholipase (PlcH, PA0844), elastase (LasB, PA3724) and pyoverdine (PA2392–2400). The three type VI secretion systems have recently been described in *P. aeruginosa* as potentially capable of targeting toxins against eukaryotes and other prokaryotes (Hood *et al.*, 2010; Basler *et al.*, 2013). Interestingly, the data revealed spatially expressed structural genes for all T6SSs as well as many effectors, which are generally up-regulated on the surface and partially in the middle of the biofilm (Supporting Information Fig. S5A). Flagella (Supporting Information Figs S4A and S5B) and pili (Supporting Information Fig. S5C) gene expressions were also spatially altered, indicating their importance for attachment and/or motility at this particular stage of biofilm growth. These data also support the general observation that the most transcriptionally active area is at the surface of the biofilm. Interestingly, the data revealed the vast majority (60–70%) of genes highly expressed throughout the biofilm have no known function (Supporting Information Fig. S1C), which warrants further investigation.

#### *Novel genes of unknown functions critically important for biofilm formation*

Surprisingly, a large proportion of unknown/hypothetical genes were up-regulated in the biofilm architecture, with higher percent biased in the interior (Supporting Information Fig. S1C), leading us to further investigate the role of these genes in biofilm formation. Many genes encoding proteins of unknown functions, clearly up-regulated in three defined spatial regions (Supporting Information Fig. S6A), were phenotypically assessed to determine whether they are critical for biofilm formation. We hypothesized that genes highly expressed in the interior of the biofilm may be essential to support the biofilm structure, prompting us to preferentially target them (Supporting Information Fig. S6A). A total of 79 unknown/hypothetical gene mutants were used in order to identify their potential role in biofilm formation (Supporting Information Fig. S6A); the majority showed a defect in biofilm formation based on the crystal violet assay (Supporting Information Fig. S6B and C). Thirteen of the mutants, showing relatively higher defects biofilm formation, were complemented and examined further (Fig. 2). Mutations in these genes significantly affected biofilm formation, as seen in both decreased biomass (Fig. 2B) and biofilm structural defects (Fig. 2C). Eleven of these thirteen genes were highly expressed in the interior of the biofilm (Fig. 2A), highlighting the importance of both unknown and previously overlooked physiological processes in this spatial niche.



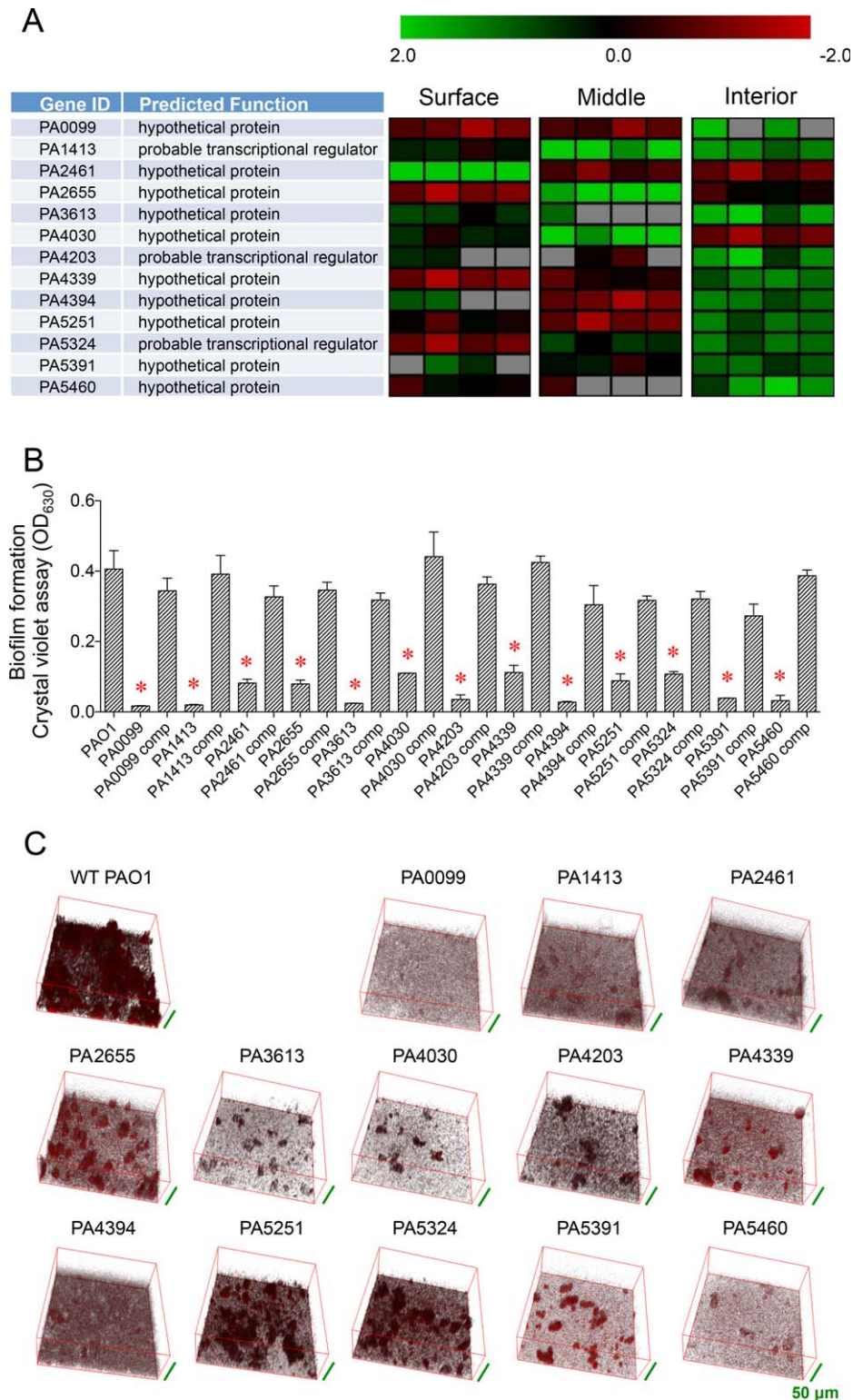


**Fig. 2.** Characterization of biofilm defective mutants.

**A.** Heat map of 13 hypothetical protein genes essential for biofilm formation. Genes were sorted according to accession numbers. Fold-changes of spatially expressed genes are shown with a red-black-green double color gradient. Green indicates up-regulation and red indicates down-regulation, as shown in the color gradient bar at the top ( $\log_2$  FC = 2 to  $-2$ ). For each location within the biofilm, the first three boxes represent the results from three biological replicates, and the fourth box represents the average fold-change of the replicates. Each biological replicate was hybridized to three microarrays and processed as technical triplicates. Grey boxes indicate no detection of transcript in at least one of the three technical triplicates.

**B.** All mutants showed significant defects in crystal violet biofilm assay, and were fully complemented by an exogenous copy of the corresponding gene inserted at the chromosomal *attTn7* site. \*,  $P < 0.05$  based on unpaired *t*-tests.

**C.** Confocal microscopy of 2 day-old *P. aeruginosa* biofilm. Biofilms of PAO1 and mutant strains were cultivated in 96-well glass bottom plates. Image stacks were obtained under 1000 $\times$  magnifications in Olympus Fluoview software and processed using ImageJ.

#### Functional assessment of biofilm-essential genes

Identifying the true mechanistic functions of hypothetical proteins, which is the ultimate goal of numerous scientists and has taken many years or careers, has

undoubtedly been extremely difficult for our group as well. We have attempted approaches to predict the functions of these hypothetical proteins critical for biofilm formation, and we will review a couple of the more direct

approaches below and their results. Multiple databases/software were utilized to attempt at deciphering the direct involvement of these 13 newly discovered genes in biofilm formation. The most reliable software, I-TASSER (Zhang, 2008; Roy *et al.*, 2010; Yang *et al.*, 2015), predicted the structure and function of these 13 hypothetical proteins (Supporting Information Fig. S8 and Table S1).

In an effort to begin understanding the direct or indirect contributions of these genes to biofilm formation, we also investigated cyclic-di-GMP levels in these 13 hypothetical protein mutant strains. Assays including pCdrA::gfp fusion (Rybtke *et al.*, 2012) and direct c-di-GMP extraction followed by LC-MS/MS analysis (Orr *et al.*, 2015) were performed for biofilm defective mutants as well as complemented strains (Supporting Information Fig. S7). Two mutants, PA1413 and PA2461, exhibited alterations in c-di-GMP levels (Supporting Information Fig. S7), which is a key intracellular metabolite in biofilm regulation (Hengge, 2009). Despite the fact that both mutants have significant defects in biofilm formation, mutant PA1413 has a decreased c-di-GMP level whereas an increased level was found in mutant PA2461 (Supporting Information Fig. S7). No conserved c-di-GMP binding signature motif was found in these two proteins, suggesting there is no direct interaction. The majority of the 13 biofilm defective mutants did not

show any alteration in the c-di-GMP levels (Supporting Information Fig. S7A). Nonetheless, these unknown proteins are shown to be critical for biofilm formation, which necessitate further *in vivo* assessment.

*Novel biofilm-essential genes contribute to in vivo fitness*

The biofilm mode of growth plays an important role in host infection, from colonization, protection against antibiotics and host defense, to establishment of chronic infection and persistence. *P. aeruginosa* biofilms have been studied extensively in both the *Drosophila melanogaster* (Mulcahy *et al.*, 2011) and the BALB/c mouse lung infection (Hoffmann *et al.*, 2005) models, which were both used to test the *in vivo* fitness of the 13 biofilm defective mutants. When introduced into these hosts, a total of nine mutants were out-competed by their corresponding complemented strains in at least one of the animal infection models (Fig. 3), suggesting a direct contribution of biofilm formation ability and *in vivo* fitness. These two models showed significantly high correlation, where a majority of the mutants (7 out of 9) are consistently less fit in both animal models (Fig. 3). All mutants that are less fit in fruit fly clearly showed an inability to attach and/or colonize the fruit fly digestive tract, with four mutants consistently correlated to

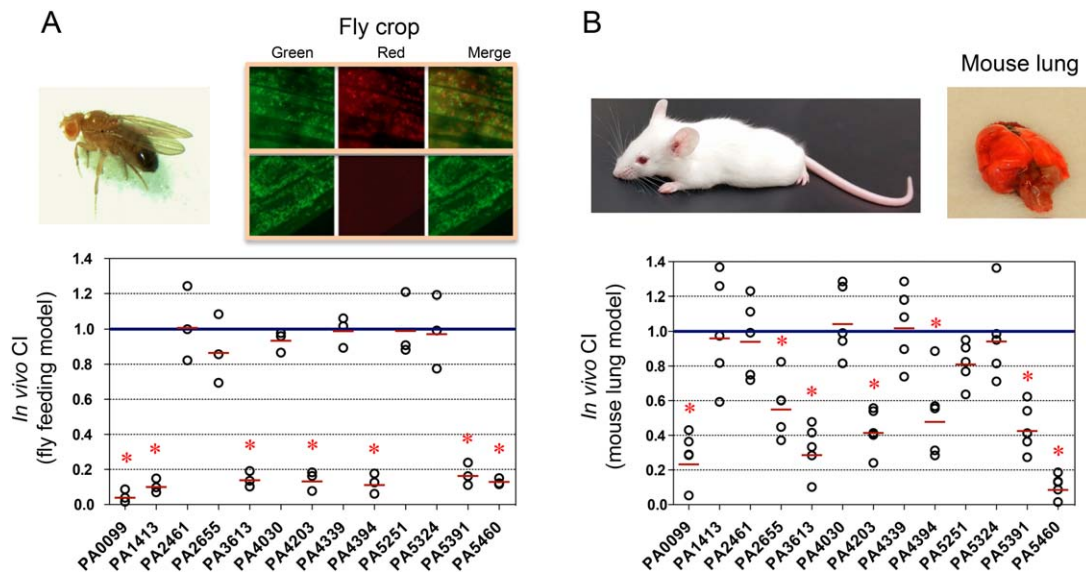


**Fig. 3.** *In vivo* competition between each mutant strain (RFP-tagged) and its corresponding complemented strain (GFP-tagged) in (A) fruit fly feeding model, and (B) BALB/c mouse lung infection model. A. Co-infection (Mulcahy *et al.*, 2011) was achieved by feeding three groups of fruit flies (5 flies in each group) with each pair of the mutant and complement strains. B. For the mouse lung infection model (Hoffmann *et al.*, 2005), groups of 5 BALB/c mice were challenged by an intratracheal infection route with each pair of strains. Post infection, the competitive index (CI) was determined using either whole fly (A) or mouse lungs (B). The solid red line represents the average CI in each competition group. CI < 1 denotes that the mutant was less competitive than its complemented strain, indicating the mutated gene is important in these hosts. \*, *P* < 0.05 based on one sample *t*-tests. Note the differences in the behavior of the PA1413 mutant in the two animal models, justifying the need to use different animal models to assess virulence.

virulence (fruit fly survival, Supporting Information Fig. S9). No *in vitro* competitive disadvantages were observed in any of these mutant strains compared to their corresponding complemented strains (Supporting Information Fig. S9), emphasizing the importance of these genes *in vivo*. Levels of many other known virulence determinants (i.e., proteases, hemolysins, lipases and rhamnolipids), the rates of planktonic growth, as well as the survival rate at stationary phase were all comparable between these mutants and the wildtype strain (Supporting Information Fig. S10). Hence, the virulence differences in flies were not a result of growth defects or overall production of other common factors such as proteases, hemolysins, lipases or rhamnolipids. It is remarkable that these seven genes were all highly expressed in the interior of the biofilm (a spatial location thought to be relatively inactive), which again, shines a spotlight on the previously unknown importance of these spatially distinct physiological processes in *in vivo* biofilm function.

## Discussion

This study is the first of its kind to utilize the published prokaryotic single-cell transcriptome technology (Kang *et al.*, 2011, 2015) for studying the functional genomics of microbial biofilms (i.e., *Pseudomonas aeruginosa*, model organism for biofilm formation). This comprehensive microarray analysis of the *P. aeruginosa* biofilm architecture showed that gene-expression of cells in the biofilm differs significantly from that in planktonic cells. Moreover, cells in unique microenvironments within in the biofilm, revealed globally by gene-expression, display markedly different behaviors. By using the planktonic bacterial gene-expression as baseline for comparison to three distinct locations in biofilm, we were able to 'tease out' essential genes for biofilm from the background.

We revealed numerous pathophysiological data of *P. aeruginosa*, including virulence and antimicrobial resistance, and discovered several novel hypothetical protein encoding genes essential for biofilm formation *in vitro* and *in vivo*. Previous studies observed that bacteria on the surface are metabolically active, while suggesting that the bacterial cells in the interior of the biofilm are behaving similarly to dormant/stationary phase bacteria (Walters *et al.*, 2003; Werner *et al.*, 2004; Rani *et al.*, 2007). This is true at the biofilm surface for many well-established pathways involved in *P. aeruginosa* pathogenesis, because our data shows significant expression of biofilm matrix components (alginate, Pel and Psl), LPS, TTSS, pyoverdine and many efflux pumps at the surface. However, the middle and interior of the biofilms

also exhibited significant gene-expression changes, with hundreds of unique genes differentially regulated. One interesting example is the up-regulated expression of the flagellar synthesis operon only in the middle of the mature biofilm. We reasoned that this expression pattern of the flagellar operon could directly correlate with the 'central hollowing detachment phenotype' observed in *P. aeruginosa* biofilm (Boles *et al.*, 2005). Additionally, many unknown/hypothetical genes were shown to be differentially expressed in three distinct locations. Part of this study attempted to identify and explore the unknown genes/pathways that are essential for biofilm formation and to assess their *in vivo* fitness and pathogenesis in two animal models. Clearly, the hurdle of identifying the mechanistic functions of hypothetical proteins involved in biofilm formation is a huge limitation, and further functional or mechanistic characterization is beyond the scope of this extensive manuscript. Hence, it is our hope and vision that the publishing of this work will recruit efforts to achieve this goal, and it presents challenges in future investigation for all in the field.

In summary, the single prokaryotic total transcript amplification technology allowed us to utilize significantly smaller sections and limited amounts of bacterial cells, which is the key contributing factor to the high resolution of transcriptomic data. Using PAO1 as the model strain, the data indicated that there are not only significant variations in global gene expressions among different locations of biofilm, but also limited yet noticeable variations among biological replicates. These observations argue for the importance of transcriptomic research, utilizing single or limited amounts of prokaryotic cells, to reveal the true heterogeneity in a population/community. It is also very likely that gene expressions within the biofilm architecture may differ among different *P. aeruginosa* strains other than PAO1 (i.e., different clinical and environmental isolates). Although the work presented here is only a snapshot of the mature biofilm transcriptome, this data set has and will further our understanding of biofilm complex pathophysiology in future investigations. We envisage that future studies of the *P. aeruginosa* temporal transcriptome, during biofilm formation and maturation, will unravel the spatiotemporal pathophysiology of biofilm communities at a global level.

## Experimental procedures

### *Bacterial strains, media and culturing conditions*

*E. coli* EPM<sub>10B</sub>-*lacI*<sup>Δ</sup>-*pir* was routinely used as a cloning strain. The *P. aeruginosa* wildtype strain, PAO1, and its derivatives were cultured in LB or biofilm minimal medium (BMM).



The biofilm was grown in a drip-flow system (Goeres *et al.*, 2009) as previously described (Lenz *et al.*, 2008) with some modifications. Briefly, BMM was prepared with 9.0 mM sodium glutamate, 50 mM glycerol, 0.25 mM MgSO<sub>4</sub>, 0.25 mM CaCl<sub>2</sub>, 0.15 mM NaH<sub>2</sub>PO<sub>4</sub>, 0.34 mM K<sub>2</sub>HPO<sub>4</sub>, 145 mM NaCl, adjusted to pH 7.0 and autoclaved. The autoclaved medium was incubated overnight at 30°C before the trace metal solution and the vitamin solution were added to the final dilutions of 50,000× or 1,000× respectively. The trace metal solution was made by dissolving 0.1 g CuSO<sub>4</sub>·5H<sub>2</sub>O, 0.1 g ZnSO<sub>4</sub>·7H<sub>2</sub>O, 0.1 g FeSO<sub>4</sub>·7H<sub>2</sub>O and 0.2 g MnCl<sub>2</sub>·4H<sub>2</sub>O in 20 ml of 0.83 M HCl. The vitamin solution contained 0.005% (w/v) thiamine and 0.00001% (w/v) biotin.

### Molecular reagents

All reagents and molecular methods used are as previously described (Kang *et al.*, 2011).

### Biofilm growth in drip-flow system with fluorescence-tagged *P. aeruginosa*

The *P. aeruginosa* wildtype strain PAO1 was labeled with green-fluorescence protein for easy visualization in the biofilm structure. Briefly, the mini-Tn7-Kan-*gfp* plasmid (Norris *et al.*, 2010) was conjugated into *P. aeruginosa* wildtype strain PAO1 along with the helper plasmid pTNS3-*asd*<sub>Ec</sub> (Kang *et al.*, 2009). *P. aeruginosa* with insertion of the mini-Tn7-Kan-*gfp* plasmid at the *attTn7* site was then selected for on LB Kan 750 µg ml<sup>-1</sup> and Triclosan 12.5 µg ml<sup>-1</sup>, and confirmed by PCR as previously described (Choi and Schweizer, 2006). This newly engineered strain, PAO1-*attTn7::mini-Tn7-Kan-gfp*, was then examined by fluorescence microscopy to confirm stable expression of the GFP protein and used for biofilm growth.

Biofilm of various *P. aeruginosa* strains were cultivated in a drip-flow chamber. All *P. aeruginosa* strains were first grown overnight in LB medium at 37°C. Bacteria were harvested, washed twice with BMM and then diluted 100× in fresh BMM. Diluted cultures were shaken at 37°C for approximately 4 h to reach an OD<sub>600</sub> of 0.2. The culture was diluted 20× in sterile saline, and 6 ml was used to inoculate each stainless-steel coupon in a drip-flow biofilm reactor chamber. After incubation at 30°C for 25 min, 1 ml of culture was removed from the chamber and fixed with 1% (w/v) paraformaldehyde for 5 min. These fixed planktonic cells served as a control in the microarray study. Sterile BMM was then pumped through the biofilm reactor chamber at 0.8 ml min<sup>-1</sup> for 72 h. Reactors were maintained at 30°C throughout the incubation, and biofilm formed on the surface of these stainless steel coupons.

### Cryosectioning of biofilm

Following incubation, coupons upon whose surface biofilm had formed were removed from the chamber and gently immersed in 1% (w/v) paraformaldehyde for 5 min. Coupons with fixed biofilm were maintained in a glass Petri

dish on dry ice, while Tissue-Tek OCT compound was applied to the surface. Once completely frozen, the biofilm was removed by slightly bending the coupon, placing it in the Petri dish back on dry ice, and then sandwiching it in OCT compound. Vertical 5 µm thick sections of the biofilm were obtained using a cryostat system, and placed onto PET membrane-coated microscope slides (PALM Micro-laser Technologies). These slides were maintained on dry ice or at -80°C until examination and sampling. Laser capture microdissection (Zeiss/PALM Laser-MicroBeam system) was used to dissect and capture biofilms sections from different vertical locations, including the surface, middle, and interior of the biofilm. Microscope slides containing the OCT-embedded biofilm sections were thawed on the microscope stage. The biofilms were then examined in DIC and green fluorescence channels at 200× magnification (e.g., Fig. 1A). Areas of the biofilms of approximately 150 µm<sup>2</sup> were laser dissected and catapulted into 2 µl of 2× lysis buffer (Kang *et al.*, 2015) in the caps of 0.2 ml PCR tubes.

### Two-color microarray and data analysis

Cells isolated from planktonic growth or biofilm were lysed, and total transcripts were amplified using our recently developed transcript amplification protocol (Kang *et al.*, 2015). The amplified ds-cDNA was labeled with Cy3 (planktonic growth) or Cy5 (biofilm) dye and hybridized to the *P. aeruginosa* 70-mer oligo arrays. Microarray images were obtained and processed as previously described (Kang *et al.*, 2011) to generate gene fold-change data ( $P \leq 0.05$ ) when comparing spatial regions of biofilm to the planktonic control. The biological replicates for each spatial region were also merged using MEV software to identify genes that are consistently up- or down-regulated ( $P \leq 0.05$ ).

### Gene assignment and pathway designation

Gene description, function prediction, and functional category assignment was assisted for some genes using the Pseudomonas Genome database (Winsor *et al.*, 2016) (<http://www.Pseudomonas.com>) and the BLAST Sequence Analysis Tool (<http://blast.ncbi.nlm.nih.gov/Blast.cgi>).

### Gene fusion construction

Twenty nine genes were chosen for validation of microarray data (Supporting Information Fig. S4). For the majority of the *gfp*-fusions (24 of 29), the *gfp*-gene was chromosomally introduced immediately downstream of each target gene as a transcriptional fusion, not disrupting any genes. A properly oriented *gfp* reporter gene with approximately 500 bp flanking regions homologous to the target gene and downstream region was generated by assembling three separate fragments in a two-step PCR. *P. aeruginosa* chromosomal DNA was first used as a template to amplify the 500 bp upstream and downstream regions, both having overlaps with the *gfp*-cassette from plasmid pPS747 (Hoang *et al.*, 1998). All three fragments were mixed in a second PCR.

The product that has the *gfp*-reporter gene with flanking homologous regions was digested with HindIII and cloned into pEX18T (Hoang *et al.*, 1998) at the HindIII site. The newly constructed plasmid was then conjugated into wild-type PAO1 strain to integrate the *gfp*-gene immediately downstream of the target genes via allelic-replacement. Strains with the desired fusion were sequentially selected first on salt free LB medium (LS) + Cb500 and then LS + 5% sucrose, and PCR confirmed with oligos annealing to outside manipulated regions on the chromosome. Five fusion strains (right panel of Supporting Information Fig. S4B) were constructed with an alternative method, because of available promoter predicted sequences. A promoter-less *gfp* gene was cloned into mini-CTX2 (Hoang *et al.*, 2000), yielding mini-CTX2-*gfp*. The upstream region of each target gene, which included the predicted promoter sequence, was PCR amplified from PAO1 genomic DNA. Each promoter region was then cloned into mini-CTX2-*gfp* upstream of the *gfp*-gene, and resulting fusion plasmids were integrated into PAO1 as previously described (Hoang *et al.*, 2000).

### Screening of biofilm essential genes

Seventy-nine genes (Supporting Information Fig. S6) that were spatially expressed differently within the biofilm architecture were screened for contribution to biofilm formation. Sixty-three mutants with individual genes insertionally disrupted were purchased from the *P. aeruginosa* Two-Allele Library (Jacobs *et al.*, 2003). The remaining 17 mutants were constructed via allelic replacement as previously described (Hoang *et al.*, 1998). All mutant strains, along with wildtype PAO1 strain as control, were first grown overnight in LB broth. All overnight cultures were diluted 100× into fresh LB and a 100 µl aliquot was inoculated into each well in a 96-well plate. Plates were covered with aluminum foil and incubated at 30°C for 48 h. Biofilm formed in the well was then stained with crystal violet and quantitated following established protocols (Merritt *et al.*, 2005). Assays were carried out in triplicate; averages are shown with standard error of the mean (S.E.M.).

Mutants that exhibited defects in ability to form wildtype level biofilm were complemented by introducing a wildtype copy of the mutated/deleted gene into the mutant strains via mini-Tn7 insertion, as previously described (Choi and Schweizer, 2006).

### Confocal microscopy

Static biofilms of RFP-labeled PAO1 and various mutant strains were cultivated in 96-well plates as described in the previous section. After 48 h, liquid medium containing planktonic bacterial cells was gently pipetted from each well. Attached biofilm was fixed with 4% (w/v) paraformaldehyde for 30 min. After fixation, paraformaldehyde was replaced with PBS and plates were examined under an Olympus FV-1000 confocal microscope on an IX-81 inverted microscope. Image stacks were obtained under 100× oil immersion in Olympus Fluoview software and processed using ImageJ software (Fig. 2).

### Quantification of intracellular c-di-GMP levels

Relative levels of c-di-GMP in *P. aeruginosa* wildtype PAO1, various mutant and complemented strains were measured using a reporter plasmid as previously described (Rybtke *et al.*, 2012). For LC-MS/MS quantification, strains were grown overnight in LB at 37°C, washed and subcultured in 1:100 in VBMM medium. Extraction of intracellular c-di-GMP and quantification using LC-MS/MS was performed as previously described (Orr *et al.*, 2015).

### Infection in animal models with biofilm defective mutants

Biofilm defective strains were used to infect *Drosophila melanogaster* Canton-S strain to investigate their abilities to colonize and replicate in flies. For easy visualization and distinguishing between the 13 mutants and their corresponding complemented strains, pUCP20-*rfp* or pUCP20-*gfp* was introduced into all mutant or complemented strains respectively. GFP- or RFP-labeled *P. aeruginosa* strains were grown separately overnight in LB+carbenicillin 500 µg ml<sup>-1</sup>. Bacteria were then harvested, washed twice with 5% sucrose, and concentrated to OD<sub>600</sub> of 25 in 5% sucrose. Concentrated bacteria cultures were then used to infect *D. melanogaster* by feeding as previously described (Mulcahy *et al.*, 2011). For fly survival curves, groups of 30 flies were infected with each of the wildtype PAO1, mutant strains, and complemented strains. Numbers of live flies were recorded at the end of each day for 14 days. An uninfected control comprised same number of flies fed with 5% sucrose only.

For the *in vivo* competitive index (CI) study, each mutant and its complemented strain were mixed at a 1:1 ratio and used for infection. At 24 h post-infection, groups of five live infected flies were homogenized in 300 µl PBS and serial dilutions were plated on LB with or without antibiotic to obtain the numbers of complemented strains, or the total numbers of bacteria respectively. These numbers were used to determine the *in vivo* CI (CFU<sub>mutant</sub>/CFU<sub>complement</sub>) when each mutant and complemented strain pair was competing in flies. Fly crops were removed and imaged under microscope in both green and red fluorescent channels at 1000× magnifications to observe fluorescent bacteria. As controls, *in vitro* CI (CFU<sub>mutant</sub>/CFU<sub>complement</sub>) was determined for each mutant/complement pair by culturing in LB medium. Statistical analysis was performed using Graphpad Prism 5.0 software.

*In vivo* competition was also performed in a different animal model, BALB/c mice, for each mutant/complemented strain pair. All animal experiments were approved by the University of Hawaii Institutional Animal Care and Use Committee (protocol No. 06–023-10), and conducted in compliance with the NIH (National Institutes of Health) Guide for the Care and Use of Laboratory Animals. Male BALB/c mice, 6–8 weeks old, were purchased from Charles River Laboratories. *In vivo* competition study was performed as previously described with some minor modifications (Kang *et al.*, 2010). Prior to infection, the mice were anesthetized by the intraperitoneal injection of 100 mg kg<sup>-1</sup> ketamine and 10 mg kg<sup>-1</sup> xylazine. Thirty milliliter of the mutant/complemented strain mixture (3 × 10<sup>7</sup> CFU of



each) resuspended in bacteria-free alginate (Hoffmann *et al.*, 2005) was inoculated intratracheally into BALB/c mice using the BioLITE Intubation System (Braintree Scientific). After 24 h, mice were humanely euthanized and lungs were harvested. Both lungs from each mouse were homogenized in 5 ml total volume of sterile saline in a Stomacher80 Biomaster tissue processor. Bacteria loads in lungs were quantified and *in vivo* CI (CFU<sub>mutant</sub>/CFU<sub>complement</sub> when grown in mouse lungs) were determined as described above for *in vivo* competition in fruit flies.

#### Detection of proteases, hemolysins, lipases and rhamnolipids

Assays for these virulence factors, including proteases, hemolysins, lipases and rhamnolipids, were performed for the mutant strains of the 13 hypothetical genes essential for biofilm formation. All assays were conducted in triplicate as previously described (Kang *et al.*, 2010), and average measurement was compared by percentage conversion relative to the wildtype PAO1 value and expressed as an average  $\pm$  S.E.M.

#### Acknowledgements

This project was supported by the US National Institutes of Health (NIH)/National Institute of General Medical Sciences (NIGMS) grant number R01GM103580, and by the Center of Biomedical Research Excellence grant P30GM114737, from the National Center for Research Resources of the National Institutes of Health. *P. aeruginosa* DNA arrays were obtained through NIAID's Pathogen Functional Genomics Resource Center, managed and funded by the Division of Microbiology and Infectious Diseases, NIAID, NIH, DHHS, and operated by the J. Craig Venter Institute. The authors declare no competing financial interests.

#### References

Basler, M., Ho, B.T., and Mekalanos, J.J. (2013) Tit-for-tat: Type VI secretion system counterattack during bacterial cell-cell interactions. *Cell* **152**: 884–894.

Billings, N., Ramirez Millan, M., Caldara, M., Rusconi, R., Tarasova, Y., Stocker, R., *et al.* (2013) The extracellular matrix component Psl provides fast-acting antibiotic defense in *Pseudomonas aeruginosa* biofilms. *PLoS Pathog* **9**: e1003526.

Boles, B.R., Thoendel, M., and Singh, P.K. (2004) Self-generated diversity produces “insurance effects” in biofilm communities. *Proc Natl Acad Sci USA* **101**: 16630–16635.

Boles, B.R., Thoendel, M., and Singh, P.K. (2005) Rhamnolipids mediate detachment of *Pseudomonas aeruginosa* from biofilms. *Mol Microbiol* **57**: 1210–1223.

Choi, K.H., and Schweizer, H.P. (2006) mini-Tn7 insertion in bacteria with single *attTn7* sites: example *Pseudomonas aeruginosa*. *Nat Protoc* **1**: 153–161.

Colvin, K.M., Gordon, V.D., Murakami, K., Borlee, B.R., Wozniak, D.J., Wong, G.C.L., *et al.* (2011) The pel polysaccharide can serve a structural and protective role in the biofilm matrix of *Pseudomonas aeruginosa*. *PLoS Pathog* **7**: e1001264.

Costerton, J.W., Lewandowski, Z., Caldwell, D.E., Korber, D.R., and Lappin-Scott, H.M. (1995) Microbial Biofilms. *Annu Rev Microbiol* **49**: 711–745.

Danielsson, D., Teigen, P.K., and Moi, H. (2011) The genital econiche: focus on microbiota and bacterial vaginosis. *Ann N Y Acad Sci* **1230**: 48–58.

Davies, D. (2003) Understanding biofilm resistance to antibacterial agents. *Nat Rev Drug Discov* **2**: 114–122.

Davies, D.G., Parsek, M.R., Pearson, J.P., Iglewski, B.H., Costerton, J.W., and Greenberg, E.P. (1998) The involvement of cell-to-cell signals in the development of a bacterial biofilm. *Science* **280**: 295–298.

Doring, G. (1997) Cystic fibrosis respiratory infections: interactions between bacteria and host defense. *Monaldi Arch Chest Dis* **52**: 363–366.

Filoche, S., Wong, L., and Sissons, C.H. (2010) Oral biofilms: emerging concepts in microbial ecology. *J Dent Res* **89**: 8–18.

Flemming, H.C., and Wingender, J. (2010) The biofilm matrix. *Nat Rev Microbiol* **8**: 623–633.

Goeres, D.M., Hamilton, M.A., Beck, N.A., Buckingham-Meyer, K., Hilyard, J.D., Loetterle, L.R., *et al.* (2009) A method for growing a biofilm under low shear at the air-liquid interface using the drip flow biofilm reactor. *Nat Protoc* **4**: 783–788.

Hengge, R. (2009) Principles of c-di-GMP signalling in bacteria. *Nat Rev Micro* **7**: 263–273.

Hoang, T.T., Karkhoff-Schweizer, R.R., Kutchma, A.J., and Schweizer, H.P. (1998) A broad-host-range Flp-*FRT* recombination system for site-specific excision of chromosomally-located DNA sequences: application for isolation of unmarked *Pseudomonas aeruginosa* mutants. *Gene* **212**: 77–86.

Hoang, T.T., Kutchma, A.J., Becher, A., and Schweizer, H.P. (2000) Integration-proficient plasmids for *Pseudomonas aeruginosa*: site-specific integration and use for engineering of reporter and expression strains. *Plasmid* **43**: 59–72.

Hoffmann, N., Rasmussen, T.B., Jensen, P.O., Stub, C., Hentzer, M., Molin, S., *et al.* (2005) Novel mouse model of chronic *Pseudomonas aeruginosa* lung infection mimicking cystic fibrosis. *Infect Immun* **73**: 2504–2514.

Hood, R.D., Singh, P., Hsu, F., Güvener, T., Carl, M.A., Trinidad, R.R.S., *et al.* (2010) A type VI secretion system of *Pseudomonas aeruginosa* targets a toxin to bacteria. *Cell Host Microbe* **7**: 25–37.

Jacobs, M.A., Alwood, A., Thaipisuttikul, I., Spencer, D., Haugen, E., Ernst, S., *et al.* (2003) Comprehensive transposon mutant library of *Pseudomonas aeruginosa*. *Proc Natl Acad Sci USA* **100**: 14339–14344.

Kang, Y., Norris, M.H., Barrett, A.R., Wilcox, B.A., and Hoang, T.T. (2009) Engineering of tellurite-resistant genetic tools for single-copy chromosomal analysis of *Burkholderia* spp. and characterization of the *B. thailandensis* *betBA*-operon. *Appl Environ Microbiol* **75**: 4015–4027.

- Kang, Y., Zarzycki-Siek, J., Walton, C.B., Norris, M.H., Hoang, T.T., and Otto, M. (2010) Multiple FadD acyl-CoA synthetases contribute to differential fatty acid degradation and virulence in *Pseudomonas aeruginosa*. *PLoS One* **5**: e13557.
- Kang, Y., Norris, M.H., Zarzycki-Siek, J., Nierman, W.C., Donachie, S.P., and Hoang, T.T. (2011) Transcript amplification from single bacterium for transcriptome analysis. *Genome Res* **21**: 925–935.
- Kang, Y., McMillan, I., Norris, M.H., and Hoang, T.T. (2015) Single prokaryotic cell isolation and total transcript amplification protocol for transcriptomic analysis. *Nat Protoc* **10**: 974–984.
- Kipnis, E., Sawa, T., and Wiener-Kronish, J. (2006) Targeting mechanisms of *Pseudomonas aeruginosa* pathogenesis. *Med Mal Infect* **36**: 78–91.
- Lappin-Scott, H., Burton, S., and Stoodley, P. (2014) Revealing a world of biofilms—the pioneering research of Bill Costerton. *Nat Rev Microbiol* **12**: 781–787.
- Lenz, A.P., Williamson, K.S., Pitts, B., Stewart, P.S., and Franklin, M.J. (2008) Localized gene expression in *Pseudomonas aeruginosa* biofilm. *Appl Environ Microbiol* **74**: 4463–4471.
- Macfarlane, S., Bahrami, B., and Macfarlane, G.T. (2011) Mucosal biofilm communities in the human intestinal tract. *Adv Appl Microbiol* **75**: 111–143.
- Mah, T.-F.C., and O'Toole, G.A. (2001) Mechanisms of biofilm resistance to antimicrobial agents. *Trends Microbiol* **9**: 34–39.
- Merritt, J.H., D.E., Kadouri and G.A., O'Toole, (2005) Growing and analyzing static biofilms. *Curr Protoc Microbiol* Chapter 1:Unit 1B.1.
- Mulcahy, H., Sibley, C.D., Surette, M.G., Lewenza, S., and Schneider, D.S. (2011) *Drosophila melanogaster* as an animal model for the study of *Pseudomonas aeruginosa* biofilm infections *in vivo*. *PLoS Pathog* **7**: e1002299.
- Norris, M.H., Kang, Y., Wilcox, B., and Hoang, T.T. (2010) Stable site-specific fluorescent tagging constructs optimized for *Burkholderia* species. *Appl Environ Microbiol* **76**: 7635–7640.
- Orr, M.W., Donaldson, G.P., Severin, G.B., Wang, J., Sintim, H.O., Waters, C.M., and Lee, V.T. (2015) Oligoribonuclease is the primary degradative enzyme for pGpG in *Pseudomonas aeruginosa* that is required for cyclic-di-GMP turnover. *Proc Natl Acad Sci USA* **112**: E5048–E5057.
- Rani, S.A., Pitts, B., Beyenal, H., Veluchamy, R.A., Lewandowski, Z., Davison, W.M., et al. (2007) Spatial patterns of DNA replication, protein synthesis, and oxygen concentration within bacterial biofilms reveal diverse physiological states. *J Bacteriol* **189**: 4223–4233.
- Roy, A., Kucukural, A., and Zhang, Y. (2010) I-TASSER: a unified platform for automated protein structure and function prediction. *Nat Protoc* **5**: 725–738.
- Rybtke, M.T., Borlee, B.R., Murakami, K., Irie, Y., Hentzer, M., Nielsen, T.E., et al. (2012) Fluorescence-based reporter for gauging cyclic di-GMP levels in *Pseudomonas aeruginosa*. *Appl Environ Microbiol* **78**: 5060–5069.
- Stewart, P.S., and Franklin, M.J. (2008) Physiological heterogeneity in biofilms. *Nat Rev Microbiol* **6**: 199–210.
- Tseng, B.S., Zhang, W., Harrison, J.J., Quach, T.P., Song, J.L., Penterman, J., et al. (2013) The extracellular matrix protects *Pseudomonas aeruginosa* biofilms by limiting the penetration of tobramycin. *Environ Microbiol* **15**: 2865–2878.
- Van Acker, H., Van Dijck, P., and Coenye, T. (2014) Molecular mechanisms of antimicrobial tolerance and resistance in bacterial and fungal biofilms. *Trends Microbiol* **22**: 326–333.
- Walters, M.C., 3rd, Roe, F., Bugnicourt, A., Franklin, M.J., and Stewart, P.S. (2003) Contributions of antibiotic penetration, oxygen limitation, and low metabolic activity to tolerance of *Pseudomonas aeruginosa* biofilms to ciprofloxacin and tobramycin. *Antimicrob Agents Chemother* **47**: 317–323.
- Werner, E., Roe, F., Bugnicourt, A., Franklin, M.J., Heydorn, A., Molin, S., et al. (2004) Stratified growth in *Pseudomonas aeruginosa* biofilms. *Appl Environ Microbiol* **70**: 6188–6196.
- Whiteley, M., Banger, M.G., Bumgarner, R.E., Parsek, M.R., Teitzel, G.M., Lory, S., and Greenberg, E.P. (2001) Gene expression in *Pseudomonas aeruginosa* biofilms. *Nature* **413**: 860–864.
- Williamson, K.S., Richards, L.A., Perez-Osorio, A.C., Pitts, B., McInerney, K., Stewart, P.S., and Franklin, M.J. (2012) Heterogeneity in *Pseudomonas aeruginosa* biofilms includes expression of ribosome hibernation factors in the antibiotic-tolerant subpopulation and hypoxia-induced stress response in the metabolically active population. *J Bacteriol* **194**: 2062–2073.
- Winsor, G.L., Griffiths, E.J., Lo, R., Dhillon, B.K., Shay, J.A., and Brinkman, F.S.L. (2016) Enhanced annotations and features for comparing thousands of *Pseudomonas* genomes in the *Pseudomonas* genome database. *Nucleic Acids Res* **44**: D646–D653.
- Xu, K.D., Stewart, P.S., Xia, F., Huang, C.T., and McFeters, G.A. (1998) Spatial physiological heterogeneity in *Pseudomonas aeruginosa* biofilm is determined by oxygen availability. *Appl Environ Microbiol* **64**: 4035–4039.
- Yang, J., Yan, R., Roy, A., Xu, D., Poisson, J., and Zhang, Y. (2015) The I-TASSER Suite: protein structure and function prediction. *Nat Methods* **12**: 7–8.
- Zhang, Y. (2008) I-TASSER server for protein 3D structure prediction. *BMC Bioinformatics* **9**: 40.

### Supporting information

Additional supporting information may be found in the online version of this article at the publisher's web-site.